

Solution Rheological Behavior and Electrospinning of Cationic Polyelectrolytes

Matthew G. McKee, Matthew T. Hunley, John M. Layman, and Timothy E. Long*

Department of Chemistry, Macromolecules and Interfaces Institute (MII), Virginia Polytechnic Institute and State University, Blacksburg, Virginia 24061

Received August 12, 2005; Revised Manuscript Received November 21, 2005

ABSTRACT: The influence of polyelectrolyte rheological behavior on the electrospinning process was determined for a series of poly(2-(dimethylamino)ethyl methacrylate hydrochloride) (PDMAEMA·HCl) aqueous solutions in the presence of added NaCl. Solution rheological studies revealed that PDMAEMA·HCl in an 80/20 w/w water/methanol cosolvent displayed polyelectrolyte behavior based on the scaling relationship between specific viscosity (η_{sp}) and concentration in the semidilute unentangled and semidilute entangled regimes. The entanglement concentration (C_e) increased with NaCl concentration due to screening of the electrostatic repulsive forces along the PDMAEMA·HCl backbone, which enabled the PDMAEMA·HCl chains to adopt a flexible, coil-like conformation. Moreover, the scaling behavior in the semidilute entangled regime shifted from polyelectrolyte ($\eta_{sp} \sim C^{1.5}$) to neutral polymer behavior ($\eta_{sp} \sim C^{3.75}$) in the high salt limit. The electrospinning performance of PDMAEMA·HCl solutions was also dependent on NaCl concentration, and NaCl-free PDMAEMA·HCl solutions did not form fibers at concentrations less than $8C_e$. The minimum concentration for fiber formation decreased as the level of NaCl was increased due to screening of the repulsive, electrostatic interactions between charged repeating units that served to stabilize the electrospinning jet. Moreover, because of the high electrical conductivity of the polyelectrolyte solutions, the electrospun polyelectrolyte fibers were 2–3 orders of magnitude smaller in diameter compared to fibers that were electrospun from solutions of neutral polymers of equal zero shear viscosity (η_0) and normalized concentration (C/C_e).

Introduction

Polyelectrolytes contain a charged atom in each repeating unit, which is balanced by a cloud of counterions in solution. Salt-free polyelectrolytes display an extended, rodlike conformation in aqueous solution due to electrostatic charge repulsion along the polymer backbone and rearrangement of counterions. Consequently, the viscoelastic behavior of polyelectrolytes differs significantly from neutral polymers.¹ In particular, polyelectrolytes exhibit a weaker scaling relationship between zero shear viscosity (η_0) and concentration compared to neutral polymers, and polyelectrolytes display enhanced shear thinning compared to neutral polymers.^{2–4} In fact, relaxation times for charged polymers in the semidilute region decrease with concentration, while relaxation times of neutral chains always increase with polymer concentration.⁵ Because of their shear thinning properties, polyelectrolytes are used as rheological additives where high shear rates are employed.⁶ Moreover, cationic polyelectrolytes are also used as emulsifiers or flocculants for wastewater treatment,⁷ and polyelectrolytes containing quaternary ammonium groups are excellent antimicrobial agents.^{8–10} More recently, cationic polyelectrolytes were explored as vectors for gene delivery due to efficient DNA complexation.¹¹

As the polyelectrolyte concentration is increased above the overlap concentration (C^*), electrostatic interactions are screened on length scales that are larger than the correlation length (ξ), and the chain is considered a random walk for length scales greater than ξ .³ Since polyelectrolytes adopt a rodlike chain conformation in dilute solution, the chain dimensions undergo greater contraction than neutral chains at intermediate concentrations between C^* and the entanglement concentration (C_e),

which increases the breadth of the semidilute unentangled regime.

The viscosity scaling relationships for polyelectrolyte solutions in the semidilute unentangled, semidilute entangled, and concentrated regimes are²

$$\begin{aligned}\eta_{sp} &\sim C^{0.5} && \text{for } C^* < C < C_e \\ \eta_{sp} &\sim C^{1.5} && \text{for } C_e < C < C_D \\ \eta_{sp} &\sim C^{3.75} && \text{for } C > C_D\end{aligned}\quad (1)$$

In eq 1, the specific viscosity is defined as $\eta_{sp} = (\eta_0 - \eta_s)/\eta_s$, where η_s is the solvent viscosity, and C_D marks the onset of the concentrated regime. As the concentration approaches the concentrated regime ($C > C_D$), the electrostatic interactions are highly screened and neutral polymer solution dynamics are recovered.² Pabon et al. observed $\eta_0 \sim C^{3.75}$ for salt-free solutions of poly(acrylamide-*co*-sodium acrylate) in the concentrated regime.¹² The addition of inorganic salts to polyelectrolyte solutions results in screening of the charged atoms along the polymer backbone.¹³ Consequently, as the electrostatic charges are screened, the charge repulsion within a polyelectrolyte is reduced and the chain becomes more coil-like. In fact, rheological scaling relationships in the semidilute entangled regime reveal a crossover from polyelectrolyte behavior ($\eta_{sp} \sim C^{1.5}$) in the absence of added salt to random coil-like, neutral polymer behavior ($\eta_{sp} \sim C^{4.6}$) at a salt concentration of 0.5 M salt concentration, which was considered the high salt limit.^{14,15}

Polyelectrolyte solutions exhibit high electrical conductivity and high net charge density due to movement of polyions and free counterions.^{16,17} An increase in net charge density was previously shown to result in smaller electrospun fiber diameters due to greater charge repulsion and plastic stretching in the

* To whom correspondence should be addressed: Tel +1-540-231-2480; Fax +1-540-231-8517; e-mail telong@vt.edu.

electrospinning jet.¹⁸ In particular, the addition of monovalent salts to neutral polymer solutions increased solution conductivity, and in general, the electrospinning process generated submicron fibers on the order of 100 nm to 10 μ m upon stretching an electrified polymer jet.¹⁹ The resulting nonwoven, fibrous mats possess a high specific surface area, submicron pores, and a high degree of porosity, which resulted in a wide range of applications including filtration devices, membranes, vascular grafts, protective clothing, molecular templates, tissue scaffolds, optical devices, and biologically functional fibers.^{20–26}

A polymer solution with sufficient chain overlap and entanglements undergoes a bending instability that causes a whiplike motion between the capillary tip and the grounded target, and this motion results in thinning of the jet and formation of submicron scale fibers.^{27,28} Fridrikh, Brenner, and Rutledge developed a model that predicts fiber diameters for several polymer solutions at various concentrations and as a function of surface tension and volume charge density.²⁹ Recent empirical correlations were developed in our laboratories that relate electrospun fiber morphology and fiber diameter to the number of chain entanglements in solution (C/C_e) where C is the polymer concentration.³⁰ This relationship was applicable for a range of molar masses and molecular architectures, including linear, randomly branched, highly branched, and star-shaped topologies. Moreover, electrospun fiber diameters were accurately predicted for several different classes of polymers, including poly(alkyl methacrylates), polyesters, and polyurethanes.³¹ Other researchers have also described the influence of chain entanglement density on electrospun fiber formation.^{32,33} In particular, Wnek et al. recently developed a semiempirical analysis that predicts the fiber morphology (beads, beaded fibers, or uniform fibers) in terms of the polymer concentration in solution, the weight-average molar mass (M_w), and the critical entanglement molar mass (M_c).³⁴

Many researchers have shown that the addition of inorganic salts to polymer solutions increases the net charge density of the electrospinning jet.^{35–39} The increase in net charge density increases the charge repulsion in the jet, thereby leading to more plastic stretching during electrospinning and the formation of thinner fibers. Moreover, the addition of salts to polymer solutions decreased the concentration of bead defects in the resulting electrospun fibers.¹⁸ This was attributed to the increase in charge repulsion along the jet and subsequent increase in surface area, which favors the formation of thinner fibers instead of beads. While solution conductivity was tailored with the addition of salt, significantly less work has focused on electrospinning charged polymers. Son et al. varied the conductivity of poly(ethylene oxide) solution upon adding small amounts (0–4 wt %) of a polyelectrolyte and studied the resulting diameter and morphology of the electrospun fibers.⁴⁰ The same researchers also studied the influence of pH on electrospinning poly(vinyl alcohol) (PVA) fibers.⁴¹ A reduction in fiber diameter was observed when electrospinning from basic PVA solutions due to larger solution conductivity. More recently, the electrospinning behavior of poly(acrylic acid) (PAA) in aqueous and DMF solutions was investigated.⁴² Unlike poly(2-(dimethylamino)ethyl methacrylate hydrochloride) (PDMAEMA·HCl) aqueous solutions, a charge is not present on each repeat unit of the PAA backbone since the fraction of the dissociated carboxylic acid groups depends on the pK_a of PAA.

In this current work PDMAEMA·HCl was electrospun in the presence of various amounts of NaCl in order to determine the role of polyelectrolyte interactions on fiber formation. Electrospun fibers that are composed of quaternary ammonium

polyelectrolytes, such as PDMAEMA·HCl, may prove useful as protective clothing since quaternary ammonium compounds serve as antimicrobial agents.⁴³ Because of the high electrical conductivity of polyelectrolyte solutions, electrospinning PDMAEMA·HCl generates submicron fibers with considerably larger specific surface areas than neutral polymers. Moreover, since the added salt ions effectively screen electrostatic interactions, a crossover from polyelectrolyte electrospinning behavior to neutral polymer electrospinning behavior may be observed in the high salt limit. Herein, the electrospinning performance of polyelectrolyte solutions with and without added salt is compared to previous empirical relationships developed for neutral, nonassociating polymers.

Experimental Section

Materials. 2-(Dimethylamino)ethyl methacrylate (DMAEMA) was purchased from Sigma Aldrich and passed through a basic alumina column in order to remove the free radical inhibitor. Ammonium persulfate initiator was also purchased from Sigma Aldrich and used as received. All other solvents and reagents were purchased from commercial sources and used without further purification.

Instrumentation. ¹H NMR spectroscopy was performed on a Varian Unity 400 spectrometer at 400 MHz in deuterium oxide. Steady shear experiments were performed with a VOR Bohlin strain-controlled solution rheometer at 25 ± 0.2 °C using a concentric cylinder geometry. The bob and cup diameters employed for rheological measurements were 14 and 15.4 mm, respectively. The rheometer was calibrated with Newtonian standard solutions. Electrospun fiber diameter and morphology were analyzed using a Leo 1550 field emission scanning electron microscope (FESEM). Fibers for FESEM analysis were collected on a 1/4 in. \times 1/4 in. stainless steel mesh, mounted on a SEM disk, and sputter-coated with an 8 nm Pt/Au layer to reduce electron charging effects. Fifty measurements on random fibers for each electrospinning condition were performed, and average fiber diameters are reported. Solution conductivities were measured with a two-electrode Oakton tester (Acorn series, model CON 6) calibrated with a 1 mS/cm standard solution from VWR Scientific.

Synthesis of PDMAEMA. DMAEMA (15 g, 95 mmol) was added to a 250 mL round-bottomed flask equipped with a magnetic stir bar, and the monomer was diluted with deionized water (60 g, 80 wt %). The monomer solution was titrated with HCl aqueous solution to a pH of 4 to protonate the monomer (DMAEMA·HCl). Finally, the ammonium persulfate initiator (15 mg, 0.1 wt % to 300 mg, 2 wt %) was added to the reaction vessel. The round-bottomed flask was equipped with a rubber septum and placed in a 60 °C oil bath. The polymerization was allowed to proceed for 24 h, and the polymer was precipitated into 1000 mL of acetone and dried under reduced pressure (0.5 mmHg) at 100 °C for 24 h. The product was characterized with ¹H NMR spectroscopy without further purification.

Electrospinning Process. PDMAEMA·HCl was dissolved in 80/20 w/w deionized water/methanol (MeOH) at various polymer concentrations. NaCl (0–50 wt % compared to the polymer) was added to the aqueous polymer solutions. The solutions were then placed in a 20 mL syringe, which was mounted in a syringe pump (KD Scientific Inc, New Hope, PA). The positive lead of a high-voltage power supply (Spellman CZE1000R; Spellman High Voltage Electronics Corp.) was connected to the 18-gauge syringe needle via an alligator clip. A grounded metal target (304 stainless steel mesh screen) was placed 20 cm from the needle tip. The syringe pump delivered the polymer solution at a controlled flow rate of 6 mL/h, and the voltage was maintained at 25 kV. It was necessary to maintain constant processing conditions to determine the role of polyelectrolyte behavior on electrospun fiber morphology and diameter.

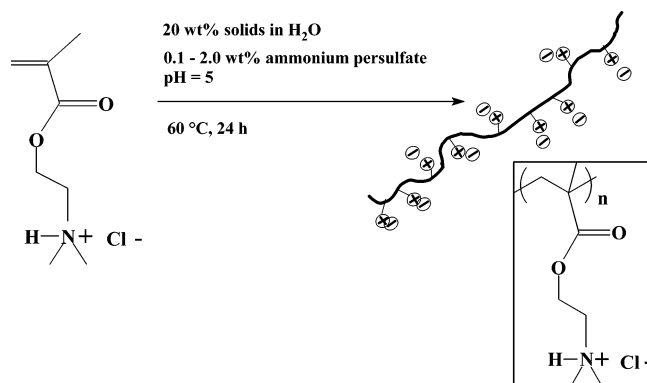


Figure 1. Synthesis of poly(2-(dimethylamino)ethyl methacrylate hydrochloride) via free radical polymerization.

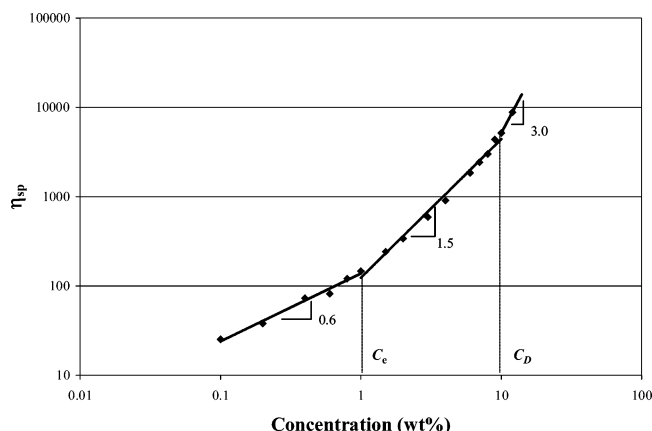


Figure 2. Dependence of η_{sp} on PDMAEMA·HCl (0.1 wt % APS) concentration.

Results and Discussion

Solution Rheology of PDMAEMA·HCl Aqueous Solutions with and without Added Salt. DMAEMA·HCl was polymerized via conventional free-radical methodologies in the presence of 0.1, 1.0, and 2.0 wt % ammonium persulfate (APS) to generate polyelectrolytes with various molar mass (Figure 1). The backbone possessed a positive charge due to the pendant quaternary amine with chlorine counterion. Unfortunately, molar mass determination via aqueous size exclusion chromatography (SEC) proved unsuccessful due to polyelectrolyte aggregation; however, a future report will describe efforts to obtain reproducible aqueous SEC measurements in the presence of various inorganic salts. All rheological and electrospinning experiments were performed with homogeneous PDMAEMA·HCl solutions in an 80/20 w/w deionized water/MeOH cosolvent, which permitted desired volatility for electrospinning.

Steady shear experiments were performed on polyelectrolyte solutions with a range of ~ 2 orders of magnitude in concentration. Specific viscosity vs concentration profiles were obtained for PDMAEMA·HCl solutions that spanned the semidilute unentangled and semidilute entangled regimes. The entanglement concentration (C_e) is the transition between the unentangled and entangled semidilute regimes and marks the solution concentration at which chains overlap sufficiently to form topologically constrained entanglements.⁴⁴ Figure 2 shows the dependence of η_{sp} on concentration for the 0.1 wt % APS PDMAEMA·HCl in an 80/20 H₂O/MeOH cosolvent. In a consistent manner with theoretical predictions for polyelectrolytes (eq 1) $\eta_{sp} \sim C^{0.6}$ in the semidilute unentangled regime, $\eta_{sp} \sim C^{1.5}$ in the semidilute entangled regime, and η_{sp} recovers the neutral polymer scaling in the concentrated regime. Both

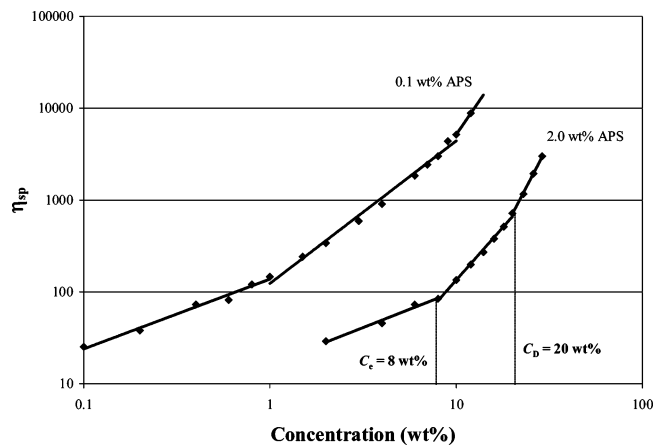


Figure 3. Influence of molar mass and concentration on the viscosity of poly(2-(dimethylamino)ethyl methacrylate hydrochloride).

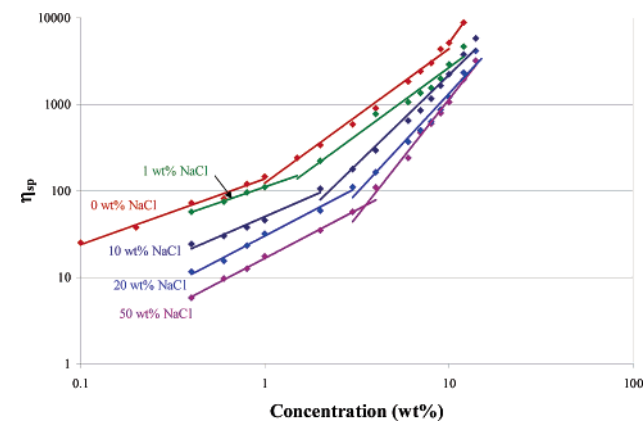


Figure 4. Effect of NaCl on polyelectrolyte solution behavior.

Table 1. Influence of NaCl on Scaling Exponents and Entanglement Concentration for PDMAEMA·HCl Solutions

NaCl concn (wt %)	semidilute unentangled exponent (a) ^a	semidilute entangled exponent (b) ^b	C_e (wt %)
0	0.6	1.5	1.0
1.0	0.7	1.6	1.5
10	0.9	2.0	2.0
20	1.1	2.5	3.0
50	1.2	3.1	3.5
neutral limit	1.25	3.75	

^a $\eta_{sp} \sim C^a$ for $C^* < C < C_e$. ^b $\eta_{sp} \sim C^b$ for $C_e < C < C_D$.

C_e and the onset of the concentrated regime (C_D) were measured over this concentration range, with values of approximately 1 and 10 wt %, respectively. In a consistent manner with predictions by Rubinstein et al.,² the slope increased at C_D because the electrostatic charges were screened in the concentrated regime due to overlap of the electrostatic blobs. The slopes in Figure 2 are in very good agreement with the theoretical predictions of polyelectrolytes ($\eta_{sp} \sim C^{0.6}$ and $\eta_{sp} \sim C^{1.5}$). Thus, it is apparent that PDMAEMA·HCl behaves as a polyelectrolyte in the 80/20 H₂O/MeOH mixed cosolvent.

Figure 3 compares the concentration dependence of η_{sp} for the 0.1 and 2.0 wt % PDMAEMA·HCl, and a qualitative comparison was obtained despite the lack of SEC molar mass information. The value of C_e increased from 1.0 to 8.0 wt %, and C_D increased from 10 to 20 wt % as the initiator concentration was increased. This is not surprising as higher molar mass chains entangle more readily than lower molar mass chains, and other researchers have also shown an inverse

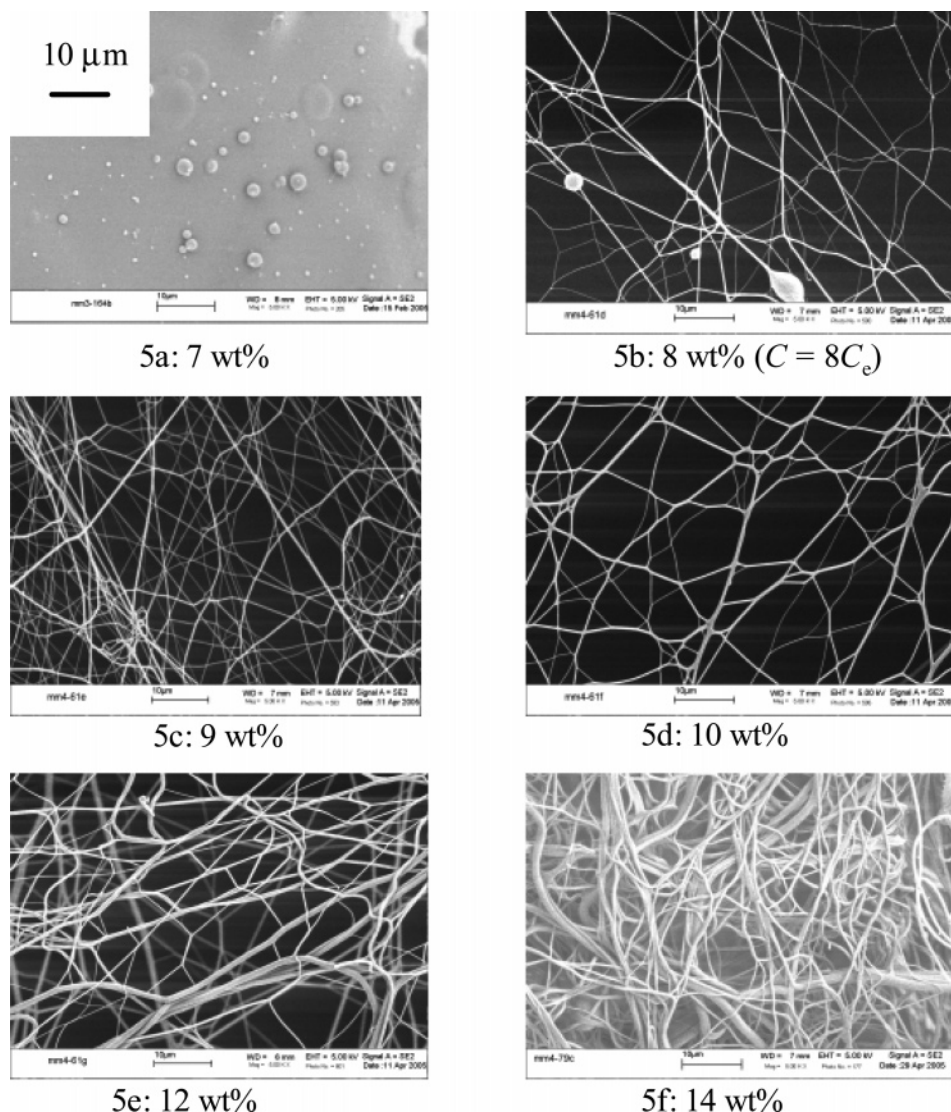


Figure 5. FESEM images of electrospun PDMAEMA·HCl fibers (0.1 wt % APS, $C_e = 1.0$ wt %) with no added salt.

relationship between C_e and polyelectrolyte chain length.⁴⁵ The slopes for the lower molar mass PDMAEMA·HCl in Figure 3 are also in excellent agreement with the scaling relationships for polyelectrolytes ($\eta_{sp} \sim C^{0.7}$ in the semidilute unentangled regime and $\eta_{sp} \sim C^{1.8}$ in the semidilute entangled regime).

Various amounts of NaCl were added to the PDMAEMA·HCl solutions to determine the influence of charge screening on the solution rheological behavior. In the high salt limit, the electrostatic interactions along a polyelectrolyte backbone are completely screened, and the scaling relationships for neutral polymers are recovered.⁴⁶ Figure 4 shows the η_{sp} of the 0.1 wt % APS PDMAEMA·HCl systematically decreased with increasing levels of NaCl in the semidilute regimes. The salt screened the electrostatic repulsive forces along the polymer backbone and enabled the PDMAEMA·HCl to adopt a flexible, coil-like conformation. Since coiled chains occupy a smaller volume in solution than extended, rodlike chains, the η_{sp} systematically decreased with NaCl addition. This viscosity dependence on salt concentration was consistent with earlier polyelectrolyte scaling relationships.⁴⁷ It is also clear from Figure 4 that at high concentrations, near C_D , the η_{sp} of the polyelectrolyte solutions with added NaCl approached the salt-free solutions. This is due to the overlap of the electrostatic blobs,

which also served to screen mutual charge repulsion along the polymer backbone. Thus, at concentrations near C_D , chain overlap and entanglements rather than salt concentration dominated the PDMAEMA·HCl solution dynamics.

The addition of NaCl also influenced the transitions between the different concentration regimes. In Figure 4, C_e systematically increased from 1.0 to 3.5 wt % as the NaCl content was increased from 0 to 50 wt % relative to PDMAEMA·HCl (Table 1). Since chains that are extended in solution occupy a larger hydrodynamic volume relative to random coiled chains, salt-free PDMAEMA·HCl formed entanglement couplings more readily with neighboring chains compared to the random coiled PDMAEMA·HCl in the presence of NaCl. The C_D transition was not measured for the solutions with added salt since C_D was outside of the concentration range investigated. It is also evident from Figure 4 that the slopes in the semidilute unentangled and semidilute entangled regimes were dependent on NaCl concentration. Table 1 summarizes the exponents in the two semidilute concentration regimes as well as the neutral scaling behavior. A gradual transition from polyelectrolyte to neutral behavior was observed for PDMAEMA·HCl with increasing salt concentration. Yamaguchi et al. also reported an increase in the concentration dependence of η_{sp} with added salt for poly(*N*-methyl-2-vinylpyridinium chloride).¹⁴

Electrospinning of PDMAEMA with Various Levels of NaCl. All polyelectrolyte solutions were electrospun at constant conditions (25 kV, 6 mL/h, and 20 cm working distance) to ensure that changes in fiber morphology and diameter were only attributed to solution properties. The solutions were electrospun from the semidilute unentangled, semidilute entangled, and concentrated regimes. The solution rheology and electrospinning trials were performed at the same conditions (room temperature, 80/20 w/w H₂O/MeOH) to ensure constant hydrodynamic dimensions of the polyelectrolytes in solution prior to experiencing the electric field. Previously, our laboratories reported that C_e was the minimum concentration which was required to electrospin beaded nanofibers for a series of linear and branched polyesters and poly(alkyl methacrylates).^{30,48,49} Consequently, the polyelectrolyte electrospinning performance was compared to the previously developed empirical relationships for these neutral, nonassociating polymers.

Figure 5 shows FESEM images of electrospun fibers that were formed from salt-free, 0.1 wt % APS PDMAEMA·HCl ($C_e = 1.0$ wt % in 80/20 H₂O/MeOH) solutions at several concentrations. At 7 wt %, polymer droplets were formed in the semidilute entangled regime (Figure 5a), in contrast to neutral polymers, which only form droplets when electrospun from the semidilute unentangled regime.³⁰ Beaded fibers with an average diameter of 120 nm were formed at 8 wt %, which corresponded to $8C_e$ (Figure 5b), and defect-free fibers with an average diameter of 170 nm were formed at 9 wt % (Figure 5c). The average fiber diameter continued to increase from 280 to 480 nm as the PDMAEMA·HCl concentration was increased from 10 to 14 wt % (Figure 5d–f). In light of correlations that were developed for neutral polymers, which predicted the formation of beaded fibers at C_e , it was surprising that PDMAEMA·HCl fibers were not obtained below $8C_e$. This observation was attributed to the relatively large conductivities of the polyelectrolyte solutions.

The size of the ions that are carried in the electrospinning jet was shown to influence the polyelectrolyte electrospinning behavior. Zong et al. reported that ions with smaller atomic radii are more mobile under an external electric field and thus impart a higher degree of stretching in the electrospinning jet.³⁶ A charged polymer possesses a significantly larger atomic radius than free salt ions, and consequently, electrospinning polyelectrolytes may result in instabilities in the electrospinning jet which may be attributed to the relative low mobility of the polyions. Thus, concentrations well above C_e are required to stabilize the electrospinning jet. Son et al. reported difficulties in electrospinning protonated poly(vinyl alcohol) (PVA) as the low mobility of the PVA polyions resulted in local variations in charge density and uneven elongation forces in the electrospinning jet.⁴⁰ The authors conjectured that the large degree of repulsion between charged groups on the chain backbone prevented the formation of a continuous jet.⁴⁰

Figure 6 shows the dependence of PDMAEMA·HCl (0.1 wt % APS) electrospun fiber diameter on normalized concentration (C/C_e). The solid black line (eq 2) is a correlation that was developed for linear and branched neutral, nonassociating polymers.³⁰

$$D [\mu\text{m}] = 0.18 \left(\frac{C}{C_e} \right)^{2.7} \quad (2)$$

The variable D is the average fiber diameter in microns. Since it was determined that C_e was the minimum concentration to form beaded fibers for neutral polymer solutions, the lower fiber diameter limit for electrospinning was ~ 180 nm. At a given value of C/C_e , PDMAEMA·HCl produced electrospun fibers

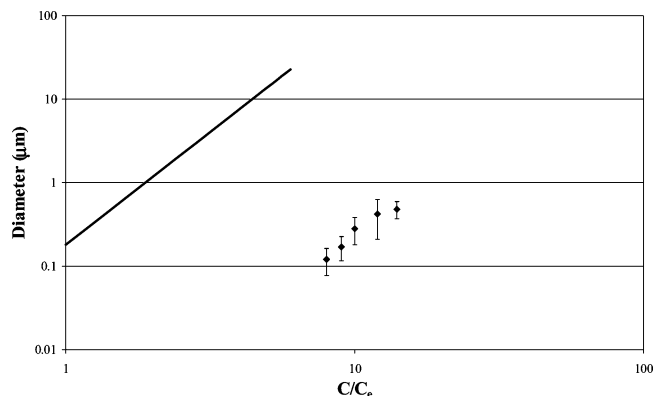


Figure 6. Dependence of polyelectrolyte fiber diameter on the normalized concentration.

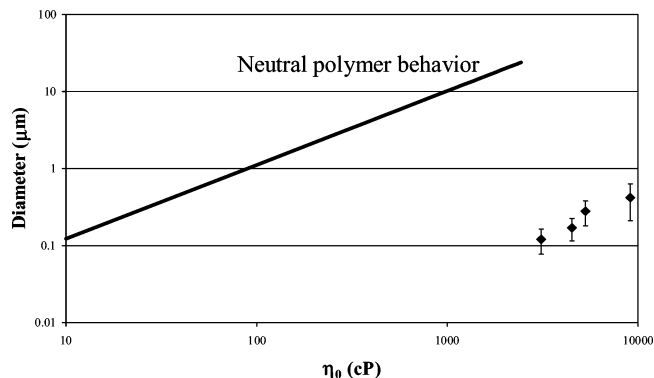


Figure 7. Effect of η_0 on electrospun fiber diameter for neutral polymers and charged polymers.

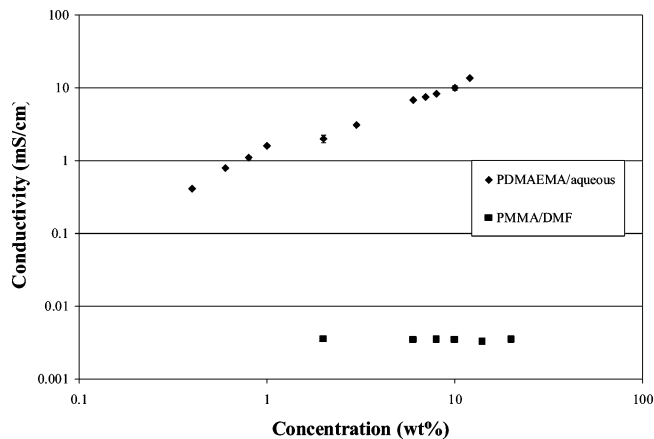


Figure 8. Effect of concentration on electrical conductivity for aqueous PDMAEMA·HCl solutions and PMMA/DMF solutions.

nearly 2 orders of magnitude smaller than the predicted value (solid black line).

Electrospun fiber diameter is also dependent on the η_0 for several different classes of polymers over a large concentration range.^{39,48} Figure 7 compares the fiber diameter– η_0 relationship between PDMAEMA·HCl and neutral polymers (solid black line). Polyelectrolyte solutions produced significantly smaller fibers than the neutral polymer solutions of equivalent η_0 due to dissociation of the PDMAEMA·HCl ions in aqueous solution. Previously, our laboratories showed slightly smaller fibers than predicted from eq 2 for poly(methyl methacrylate-*co*-methacrylic acid) (PMMA-*co*-PMAA) solutions in dimethylformamide.⁴⁸ This was attributed to partial dissociation of the carboxylic acid group, which resulted in a higher conductivity in the jet and greater charge repulsion during electrospinning. In fact, the

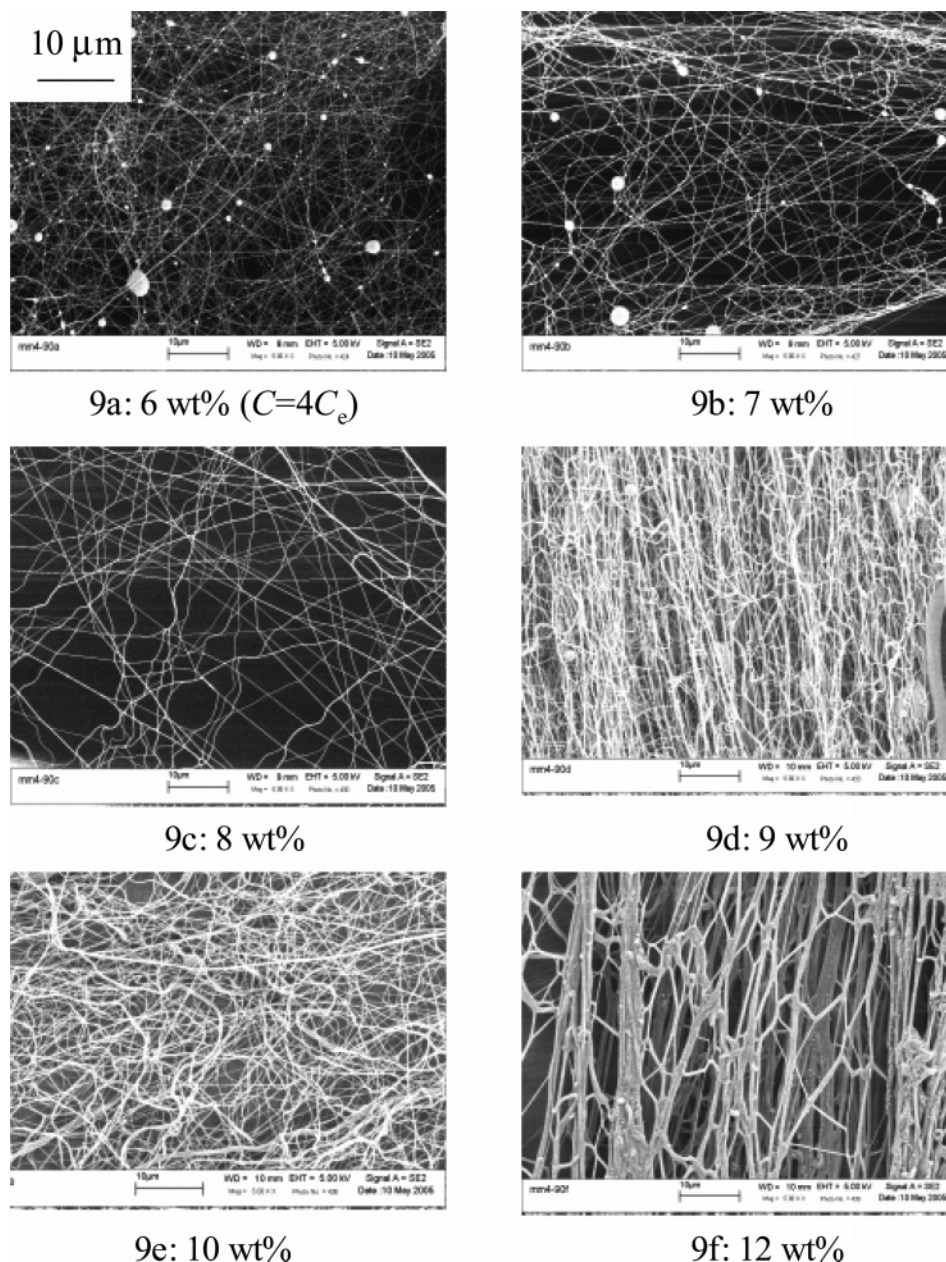


Figure 9. FESEM images of electrospun PDMAEMA·HCl fibers (0.1 wt % APS, $C_e = 1.5$ wt %) with 1 wt % added NaCl.

PMMA-*co*-PMAA solutions displayed electrical conductivities nearly an order of magnitude greater than the poly(methyl methacrylate) (PMMA) control in the identical solvent. Similarly, the PDMAEMA·HCl aqueous solutions had very high electrical conductivities relative to the neutral polymer solutions, which resulted in a higher degree of elongation during electrospinning and formation of thinner fibers. Thus, it may be advantageous to electrospin polyelectrolytes rather than neutral polymers for applications demanding high specific surface area.

Figure 8 shows the concentration dependence of electrical conductivity for PDMAEMA·HCl (0.1 wt % APS). A concentration series of PMMA in DMF was included since eq 2 was developed from electrospinning neutral polymer solutions with conductivities on the order of the PMMA/DMF solutions. The electrical conductivity of the PDMAEMA·HCl polyelectrolyte solution was nearly 3 orders of magnitude larger than the neutral PMMA solution. In contrast to the PMMA solution, the conductivity of the PDMAEMA·HCl solution was also dependent on concentration due to an increase in charge density with polyelectrolyte concentration. This explained the significant

reduction in polyelectrolyte fiber diameter compared to predictions in Figures 6 and 7.

PDMAEMA·HCl solutions were also doped with different levels of NaCl relative to the polyelectrolyte concentration to determine the role of screening electrostatic interactions on electrospinning performance. Figure 9 shows FESEM images of PDMAEMA·HCl electrospun with 1 wt % NaCl at several different concentrations. As described in section 3.1, C_e increased from 1 to 1.5 wt % upon increasing NaCl from 0 to 1 wt %. The minimum concentration that was required to form electrospun fibers was 6 wt %, or $4C_e$ (Figure 9a). The average fiber diameter that was reproducibly formed from the 6 wt % solution was 60 nm. The addition of 1 wt % NaCl shifted the minimum concentration for fiber formation closer to C_e , which is the minimum concentration for fiber formation for neutral polymers.³⁰ This was attributed to a reduction in electrostatic charge repulsion along the polymer backbone, which served to stabilize the electrospinning jet. Beaded fibers ~90 nm in diameter were formed at 7 wt % (Figure 9b), while uniform, bead-free fibers were produced at 8 wt % (Figure 9c). As the

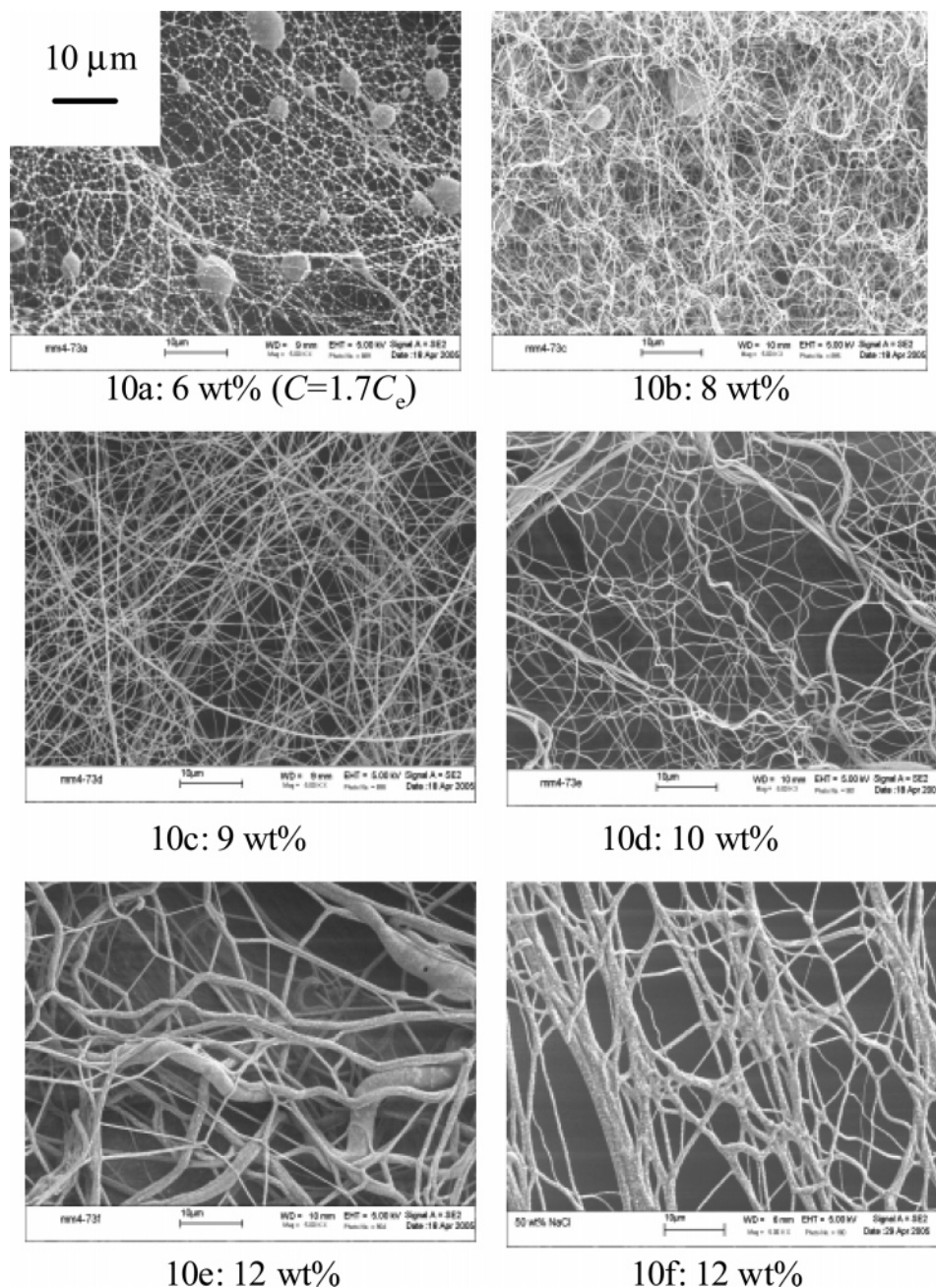


Figure 10. FESEM images of electrospun PDMAEMA·HCl fibers (0.1 wt % APS, $C_e = 3.5$ wt %) with 50 wt % added NaCl.

concentration was increased from 9 to 10 wt %, the average fiber diameter further increased from 160 to 290 nm (Figure 9d,e). Finally, at 12 wt % the average electrospun fiber diameter was 600 nm (Figure 9f). Moreover, NaCl crystals appeared on the fiber surface as shown in Figure 9f.

Figure 10 shows FESEM images of PDMAEMA·HCl fibers that were electrospun with 50 wt % added NaCl. The $\eta_{sp}-C$ scaling exponents in Table 1 show that the neutral scaling behavior was approximately recovered at 50 wt % NaCl, which indicated that nearly all electrostatic charges were screened. The minimum concentration for fiber formation was 6 wt % (Figure 10a), or $1.7C_e$, which is significantly closer to neutral polymer behavior than in Figures 5 and 9. Thus, as the NaCl level was increased, the electrospinning behavior of the polyelectrolyte solution shifted toward behavior that was expected of an uncharged polymer. Beaded fibers with ~ 130 nm in diameters were produced when PDMAEMA·HCl with 50 wt % added NaCl was electrospun at 8 wt % (Figure 10b), while uniform

Table 2. Influence of NaCl on Electrospun Fiber Formation

NaCl concn (wt %)	C/C_e at onset of fiber production	η_0 (cP) at onset of fiber production
0	8.0	2500
1.0	4.0	1100
10	3.5	880
20	2.3	520
50	1.7	100
neutral limit	1.0	~ 20

fibers (~ 260 nm) were produced at 9 wt % (Figure 10c). The average fiber diameter systematically increased from 300 nm to $1.2 \mu\text{m}$ (Figure 10d–f) as the concentration was increased from 10 to 14 wt %. It should be noted that there is a relatively large distribution of fiber diameters at the higher concentrations (Figure 10e,f).

Table 2 summarizes the electrospinning behavior of PDMAEMA·HCl with various levels of NaCl and provides a comparison to neutral polymer behavior. In particular, the

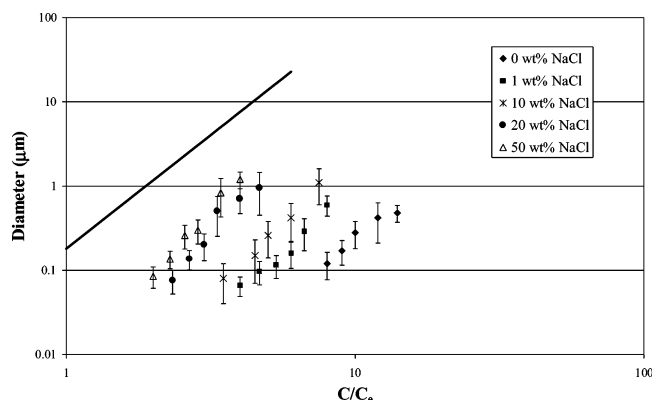


Figure 11. Influence of NaCl on the average electrospun fiber diameter dependence on the normalized concentration.

minimum normalized concentration and the η_0 at which fiber formation occurred are presented. A systematic trend toward neutral polymer electrospinning behavior was evident as the NaCl concentration was increased. As mentioned previously, concentrations well above C_e were required to electrospin fibers from the salt-free polyelectrolyte solutions, due to the large degree of repulsion between charged sites on the polyelectrolyte backbone. Consequently, high-viscosity solutions ($C > C_e$) were necessary to form a stable jet.

Figure 11 shows the influence of NaCl on the electrospun fiber diameter dependence on the normalized concentration. The solid black line represents the electrospinning behavior of neutral polymer solutions, as defined in eq 2. As mentioned previously, PDMAEMA·HCl formed thinner fibers at an equivalent C/C_e than predicted due to the large solution conductivity of polyelectrolytes and high degree of charge repulsion in the electrospinning jet (Figure 8). For a given value of C/C_e , the average fiber diameter increased with NaCl addition. Moreover, as the salt concentration was raised from 0 to 20 wt %, the fiber diameter dependence on C/C_e shifted to the neutral polymer relationship (eq 2). The electrostatic repulsive interactions between charged groups were progressively screened as the NaCl was increased, which decreased the stretching in the electrospinning jet and increased the fiber diameter. Figure 11 indicates that the electrospun fiber diameter was insensitive to salt concentrations that were greater than 20 wt %, which indicated that the majority of polyelectrolyte electrostatic interactions were screened at high salt concentrations. These results are in qualitative agreement with results from Kim et al., who observed an increase in poly(acrylic acid) fiber diameter in the presence of NaCl.⁵⁰

The conductivity of the PDMAEMA·HCl (0.1 wt % APS) solutions increased slightly with NaCl concentration due to an increased ion content (Figure 12). Bordi et al. also showed an increase in electrical conductivity with added NaCl for a series of aqueous poly(acrylic acid) solutions.⁵¹ Higher solution conductivity generally results in thinner electrospun fibers. However, the PDMAEMA·HCl average fiber diameter actually increased with NaCl concentration due to the competing effect of electrostatic screening. Electrostatic screening reduced the charge repulsion in the electrospinning jet and ultimately decreased the degree of stretching. Li and Hsieh recently observed similar behavior when electrospinning poly(acrylic acid) solutions with added salt.⁴² It should be noted that even at very high NaCl levels of 50 wt %, the neutral polymer behavior was not completely recovered (Figure 11). The electrical conductivity was still 3–4 orders of magnitude larger for the PDMAEMA·HCl polyelectrolytes compared to the

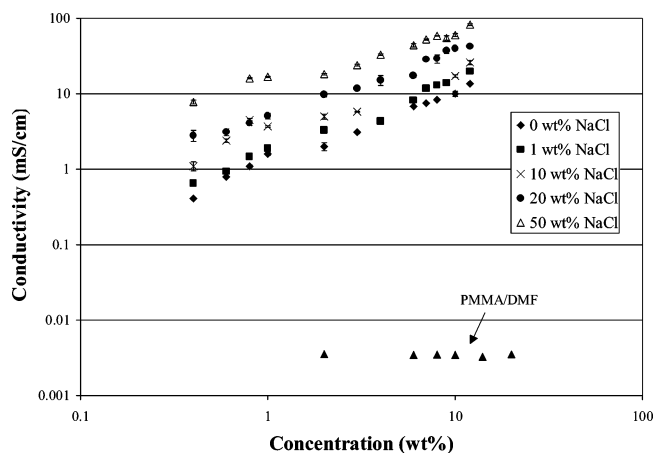


Figure 12. Influence of NaCl concentration on PDMAEMA·HCl solution conductivity.

neutral polymer solutions, and thinner fibers were produced at an equivalent C/C_e .

Conclusions

The electrospinning behavior and influence of NaCl addition were studied for a series of PDMAEMA·HCl 80/20 w/w H₂O/MeOH solutions. The aqueous PDMAEMA·HCl solutions displayed classic polyelectrolyte behavior with $\eta_{sp} \sim C^{0.6}$ in the semidilute unentangled regime and $\eta_{sp} \sim C^{1.5}$ in the semidilute entangled regime. As expected, C_e systematically increased with NaCl concentration as the extended, rodlike chains adopted a random, coillike conformation. Furthermore, the scaling behavior in the semidilute entangled regime shifted from polyelectrolyte ($\eta_{sp} \sim C^{0.5}$) to neutral polymer behavior ($\eta_{sp} \sim C^{3.75}$) in the high salt limit. While neutral polymer solutions produce beaded electrospun fibers at C_e , salt-free PDMAEMA·HCl solutions did not form fibers at concentrations less than $8C_e$. The minimum concentration for fiber formation decreased to $1.5C_e$ as the concentration of NaCl was increased to 50 wt %. This decrease was attributed to screening of the repulsive, electrostatic interactions that stabilize the electrospinning jet. Moreover, because of the large electrical conductivity of the polyelectrolyte solutions, the average diameters of the polyelectrolyte fibers significantly smaller compared to neutral polymer solutions of equal η_0 and normalized concentration (C/C_e). These ultrafine electrospun PDMAEMA·HCl fibers may prove useful in protective clothing applications for chemical and biological agents as quaternary ammonium compounds are known antimicrobial agents.

Acknowledgment. This material is based upon work supported by the U.S. Army Research Laboratory and the U.S. Army Research Office under Contract/Grant DAAD19-02-1-0275 Macromolecular Architecture for Performance Multi-disciplinary University Research Initiative (MAP MURI). The authors also gratefully acknowledge Dr. Cheryl Heisey from the Department of Chemistry at Virginia Tech for a critical review of this manuscript.

References and Notes

- (1) Muthukumar, M. *J. Chem. Phys.* **1997**, *107*, 2619–2635.
- (2) Rubinstein, M.; Colby, R. H.; Dobrynin, A. V. *Phys. Rev. Lett.* **1994**, *73*, 2776–2779.
- (3) Dobrynin, A. V.; Colby, R. H.; Rubinstein, M. *Macromolecules* **1995**, *28*, 1859–1871.
- (4) Chen, S.-P.; Archer, L. A. *J. Polym. Sci., Part B: Polym. Phys.* **1999**, *37*, 825–835.

- (5) Krause, W. E.; Tan, J. S.; Colby, R. H. *J. Polym. Sci., Part B: Polym. Phys.* **1999**, *37*, 3429–3437.
- (6) Zhang, L.-M.; Tan, Y.-B.; Li, Z.-M. *Colloid Polym. Sci.* **1999**, *277*, 1001–1004.
- (7) Fernandes, R. S.; Gonzalez, G.; Lucas, E. F. *Colloid Polym. Sci.* **2005**, *283*, 375–382.
- (8) Kenawy, E.-R.; Malmoud, Y. A. G. *Macromol. Biosci.* **2003**, *3*, 107–116.
- (9) Cakmuk, I.; Ulukanli, Z.; Tuzcu, M.; Karabuga, S.; Genctav, K. *Eur. Polym. J.* **2004**, *40*, 2373–2379.
- (10) Grunian, J. C.; Choi, J. K.; Lin, A. *Biomacromolecules* **2005**, *6*, 1149–1153.
- (11) Smedt, S. C.; Demeester, J.; Hennink, W. E. *Pharm. Res.* **2000**, *17*, 113–126.
- (12) Pabon, M.; Selb, J.; Candau, F. *Langmuir* **1998**, *14*, 735–737.
- (13) Boris, D. C.; Colby, R. H. *Macromolecules* **1998**, *31*, 5746–5755.
- (14) Yamaguchi, M.; Wakutsu, M.; Takahashi, Y.; Noda, I. *Macromolecules* **1992**, *25*, 470–474.
- (15) Yamaguchi, M.; Wakutsu, M.; Takahashi, Y.; Noda, I. *Macromolecules* **1992**, *25*, 475–478.
- (16) Bordini, F.; Colby, R. H.; Cametti, C.; De Lorenzo, L.; Gill, T. J. *Phys. Chem. B* **2002**, *106*, 6887–6893.
- (17) Colby, R. H.; Boris, D. C.; Krause, W. E.; Tan, J. S. *J. Polym. Sci., Part B: Polym. Phys.* **1997**, *35*, 2951–2969.
- (18) Fong, H.; Chun, I.; Reneker, D. H. *Polymer* **1999**, *40*, 4585–4592.
- (19) Reneker, D. H.; Chun, I. *Nanotechnology* **1996**, *7*, 216–223.
- (20) Li, D.; Xia, Y. *Adv. Mater.* **2004**, *16*, 1151–1170.
- (21) Gibson, P.; Schreuder-Gibson, H.; Rivin, D. *Colloids Surf., A* **2001**, *187*, 187–188, 469–481.
- (22) Kim, K.; Yu, M.; Zong, X.; Chiu, J.; Fang, D.; Seo, Y.-S.; Hsiao, B. S.; Chu, B.; Hadjiargyrou, M. *Biomaterials* **2003**, *24*, 4977–4985.
- (23) Kenawy, E.-R.; Bowlin, G. L.; Mansfield, K.; Layman, J.; Simpson, D. G.; Sander, E. H.; Wnek, G. E. *J. Controlled Release* **2002**, *81*, 57–64.
- (24) Yoshimoto, H.; Shin, Y. M.; Terai, H.; Vacanti, J. P. *Biomaterials* **2003**, *24*, 2077–2082.
- (25) Wang, X.; Drew, C.; Lee, S.-H.; Senecal, K. J.; Kumar, J.; Samuelson, L. A. *Nano Lett.* **2002**, *2*, 1273–1275.
- (26) Casper, C. L.; Yamaguchi, N.; Kiick, K. L.; Rabolt, J. F. *Biomacromolecules* **2005**, *6*, 1998–2007.
- (27) Reneker, D. H.; Yarin, A. A.; Fong, H.; Koombhongse, S. *J. Appl. Phys.* **2000**, *87*, 4531–4547.
- (28) Shin, Y. M.; Hohman, M. M.; Brenner, M. P.; Rutledge, G. C. *Polymer* **2001**, *42*, 9955–9967.
- (29) Fridrikh, S. V.; Yu, J. H.; Brenner, M. P.; Rutledge, G. C. *Phys. Rev. Lett.* **2003**, *90*, Art No. 144502.
- (30) McKee, M. G.; Wilkes, G. L.; Colby, R. H.; Long, T. E. *Macromolecules* **2004**, *37*, 1760–1767.
- (31) McKee, M. G.; Park, T.; Unal, S.; Yilgor, I.; Long, T. E. *Polymer* **2005**, *46*, 2011–2015.
- (32) Koski, A.; Yim, K.; Shivkumar, S. *Mater. Lett.* **2004**, *58*, 493–497.
- (33) Gupta, P.; Elkins, C.; Long, T. E.; Wilkes, G. L. *Polymer* **2005**, *46*, 4799–4810.
- (34) Shenoy, S. L.; Bates, W. D.; Frisch, H. L.; Wnek, G. E. *Polymer* **2005**, *46*, 3372–3384.
- (35) Subbiah, T.; Bhat, G. S.; Tock, R. W.; Parameswaran, S.; Ramkumar, S. S. *J. Appl. Polym. Sci.* **2005**, *96*, 557–569.
- (36) Zong, Z.; Kim, K.; Fang, D.; Ran, S.; Ran, S.; Hsiao, B.; Chu, B. *Polymer* **2002**, *43*, 4403–4412.
- (37) Demir, M. M.; Yilgor, I.; Yilgor, E.; Erman, B. *Polymer* **2002**, *43*, 3303–3309.
- (38) Jun, Z.; Hou, H.; Schaper, A.; Wendroff, J. H.; Greiner, A. *e-Polym.* **2003**, no. 009.
- (39) Mit-uppatham, C.; Nithitanakul, M.; Supaphol, P. *Macromol. Chem. Phys.* **2004**, *205*, 2327–2338.
- (40) Son, W. K.; Youk, J. H.; Lee, T. S.; Park, W. H. *Polymer* **2004**, *45*, 2959–2966.
- (41) Son, W. K.; Youk, J. H.; Lee, T. S.; Park, W. H. *Mater. Lett.* **2005**, *59*, 1571–1575.
- (42) Li, L.; Hsieh, Y.-L. *Polymer* **2005**, *46*, 5133–5139.
- (43) Boulmedais, F.; Frisch, B.; Etienne, O.; Lavalle, Ph.; Picart, C.; Ogier, J.; Voegel, J.-C.; Schaaf, P.; Egles, C. *Biomaterials* **2004**, *25*, 2003–2011.
- (44) Krause, W. E.; Bellomo, E. G.; Colby, R. H. *Biomacromolecules* **2001**, *2*, 63–69.
- (45) Di Cola, E.; Plucktaveesak, N.; Waigh, T. A.; Colby, R. H.; Tan, J. S.; Pyckhout-Hintzen, W.; Heenan, R. K. *Macromolecules* **2004**, *37*, 8457–8465.
- (46) Lauten, R. A.; Nystrom, B. *Macromol. Chem. Phys.* **2000**, *201*, 677–684.
- (47) Konop, A. J.; Colby, R. H. *Macromolecules* **1999**, *32*, 2803–2805.
- (48) McKee, M. G.; Elkins, C. L.; Long, T. E. *Polymer* **2004**, *45*, 8705–8715.
- (49) McKee, M. G.; Long, T. E. *Polym. Prepr. (Am. Chem. Soc., Div. Polym. Chem.)* **2004**, *45*, 130–131.
- (50) Kim, B.; Park, H.; Lee, S.-H.; Sigmund, W. M. *Mater. Lett.* **2005**, *59*, 829–832.
- (51) Bordini, F.; Cametti, C.; Gili, T. *Phys. Rev. E* **2003**, *68*, Art No. 011805.

MA051786U